

Tailoring superradiance to design artificial quantum systems

Paolo Longo,* Christoph H. Keitel, and Jörg Evers†

Max Planck Institute for Nuclear Physics, Saupfercheckweg 1, 69117 Heidelberg, Germany

(Dated: March 2, 2022)

Cooperative phenomena arising due to the coupling of individual atoms via the radiation field are a cornerstone of modern quantum and optical physics. Recent experiments on x-ray quantum optics added a new twist to this line of research by exploiting superradiance in order to construct artificial quantum systems. However, so far, systematic approaches to deliberately design superradiance properties are lacking, impeding the desired implementation of more advanced quantum optical schemes. Here, we develop an analytical framework for the engineering of single-photon superradiance in extended media applicable across the entire electromagnetic spectrum, and show how it can be used to tailor the properties of an artificial quantum system. This “reverse engineering” of superradiance not only provides an avenue towards non-linear and quantum mechanical phenomena at x-ray energies, but also leads to a unified view on and a better understanding of superradiance across different physical systems.

A single atom coupled to an environment is usually subject to spontaneous emission and experiences a frequency shift referred to as the Lamb shift. In an aggregation of atoms coupled via the radiation field, collective effects can significantly alter the properties compared to a single emitter. For instance, this was realised by Dicke [1, 2], who showed that N identical atoms confined to a volume much smaller than a wavelength cubed collectively behave as one “super atom”. This leads to exaggerated properties such as an acceleration of spontaneous decay by a factor of $\chi_{\text{Dicke}} = N$ (known as superradiance) or an enhanced frequency shift (sometimes also termed “collective Lamb shift”). Recently, also the correlated emission from *extended* ensembles of emitters has become the focus of experimental and theoretical [3–5] investigations, where either the system size and/or the minimal interatomic distance a exceeds the scale of the characteristic wavelength λ_0 . The systems considered cover a wide range of possible realisations, including atoms near a nanofiber [6], thin vapor layers [7], cold atomic ensembles [8–12], or thin-film cavities with embedded Mössbauer nuclei in the realm of x-ray quantum optics [13–20].

The present work is motivated by the observation that in particular the latter experiments in the field of nuclear quantum optics exploited a deliberate control of superradiance properties, going beyond a mere characterisation. For instance, the observation of electromagnetically induced transparency at x-ray frequencies [13] was enabled by the engineering of two distinct ensembles with different superradiance properties in a single sample. Another example is the implementation of spontaneously generated coherences [14], which relied on the realization of a spatially anisotropic electromagnetic environment via superradiance. In both cases, superradiance was employed to design an artificial quantum system, which in turn enabled the observation of the desired effect.

This raises the question whether a systematic and constructive approach could be established to exploit superradiance for the design of artificial quantum systems. Such design capabilities could overcome the limited resources accessible in state-of-the-art experiments, and thereby enable more advanced level schemes required, e.g., for the exploration of non-linear and quantum effects at x-ray energies.

Here, we address this question by developing an analytical framework for superradiance in extended media encompassing different system dimensionalities, interatomic couplings, and environments. As our main result, we then derive expressions describing how collective decay rates and frequency shifts can be controlled in extended media, and show how they can be used for the design of an artificial optical transition.

We start with a single two-level atom (bare transition frequency $\omega_0 = ck_0$, $k_0 = 2\pi/\lambda_0$, c is the speed of light) which is embedded in an electromagnetic environment (e. g., free space) and is characterised by its spontaneous decay rate $\text{Re}(V_0) \equiv \gamma_0$ (assuming Markovian reservoirs [21]). The coupling to the environment also results in a frequency shift $\text{Im}(V_0)/2 \equiv \delta\omega_0$ (single-atom Lamb shift). In the presence of an identical, second atom, photons can be exchanged between the two atoms. Due to irreversible loss to the reservoir, the inter-atomic coupling $V_{\mathbf{r}_i\mathbf{r}_j} = \gamma_{\mathbf{r}_i\mathbf{r}_j} + 2i\delta\omega_{\mathbf{r}_i\mathbf{r}_j}$ is complex [21–25]. Here, $\gamma_{\mathbf{r}_i\mathbf{r}_j}$ ($\delta\omega_{\mathbf{r}_i\mathbf{r}_j}$) represents the real-valued cross-damping (cross-coupling) term for two atoms located at positions \mathbf{r}_i and \mathbf{r}_j , respectively. Considering all pair-wise couplings in an ensemble of $N \gg 1$ atoms, we find [22, 24]

$$0 = -\frac{i}{2} \sum_{j=1}^N V_{\mathbf{r}_i\mathbf{r}_j} \varphi_{\mathbf{r}_j} - (E - \omega_0) \varphi_{\mathbf{r}_i}, \quad (1)$$

* paolo.longo@mpi-hd.mpg.de

† joerg.evers@mpi-hd.mpg.de

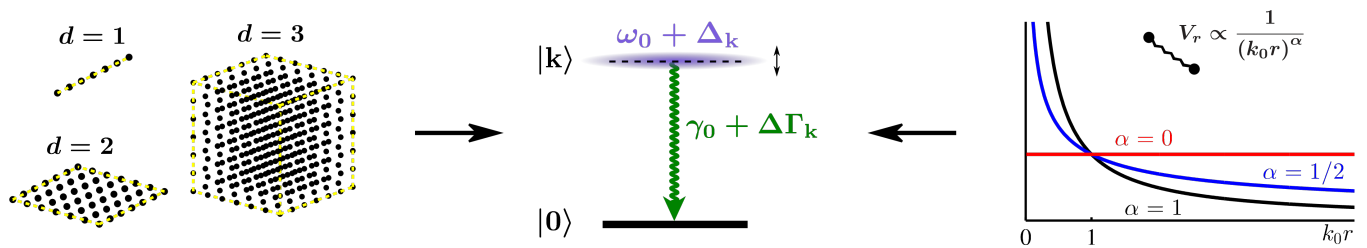


Figure 1. **Design of an artificial optical transition through tailored superradiance.** A d -dimensional lattice of atoms is embedded into an electromagnetic reservoir that mediates an inter-atomic coupling $V_r \propto 1/r^\alpha$, where atoms are separated by a distance r and the coefficient α characterises the distance-dependence (see eq. (2)). We show that the resulting collective eigenstates can be utilised for the implementation of an artificial transition with tunable decay rate and transition frequency.

where E denotes the complex eigenenergy of the collective single-excitation atomic state $|\Psi\rangle = \sum_{i=1}^N \varphi_{\mathbf{r}_i} \sigma_i^+ |0\rangle$ (σ_i^+ and $|0\rangle$ signify the atomic raising operator for atom i and the vacuum state, respectively). Equation (1) is valid for all dimensions d of the atomic arrangement and for all (physically reasonable) couplings $V_{\mathbf{r}_i \mathbf{r}_j}$. Collective decay rates and frequency shifts are obtained via $\Gamma \equiv -2\text{Im}(E)$ and $\Delta \equiv \text{Re}(E) - \omega_0$, respectively [22, 24].

In Dicke's small-volume limit, all atoms couple to each other with equal strength, leading to a collective decay rate $\Gamma = N\gamma_0 = \chi_{\text{Dicke}}\gamma_0$ and a frequency shift $\Delta = \chi_{\text{Dicke}}\delta\omega_0$ with an enhancement factor χ_{Dicke} (see methods). To describe an extended sample, we consider ordered atomic arrangements, and focus on chains ($d = 1$), square lattices ($d = 2$), and simple cubic lattices ($d = 3$), see fig. 1. The smallest inter-atomic distance is given by the lattice constant a . Such ordered arrays are naturally provided by crystalline samples (e. g., solid state targets employed in x-ray quantum optics [13–18], optical lattices of atoms [26], or atom–cavity networks [27]). Furthermore, we consider a generic class of inter-atomic couplings

$$\frac{V_r}{\gamma_0} = A_d \sin^2 \theta \frac{e^{i\epsilon k_0 r}}{(k_0 r)^\alpha} \quad (\alpha \geq 0, \epsilon = \pm), \quad (2)$$

which depend on the distance r between atom pairs. Here, the coefficient α classifies the distance-dependence and A_d is a dimensionless coupling strength. We also assume the atomic dipole moments to be uniformly aligned along the x_3 axis. This orientation dependence is taken into account by the angle θ (see methods for further details). Since multiple terms of type (2) can be accounted for by a linear combination, in particular also the three common implementations of three-dimensional free space [22], atoms confined to two spatial dimensions [28], or atoms coupled to a one-dimensional waveguide [29] are covered. The coupling parameters for these three examples are specified in table 1. Note that in principle α can be artificially engineered and controlled as has recently been demonstrated at optical frequencies [10].

RESULTS AND DISCUSSION

The solution of eigenproblem (1) (see methods) reveals that those eigenstates $|\mathbf{k}\rangle$ whose wavevector's magnitude matches the wavenumber set by the single atom transition, i. e., $k = |\mathbf{k}| = k_0$, exhibit the maximum possible decay rate $\Gamma_{\text{max}} = \chi_{\text{max}}\gamma_0$ if the constraint

$$0 \leq \alpha < \frac{d+1}{2} \quad (3)$$

is fulfilled. This criterion is a necessary condition for the emergence of superradiance and represents bounds on the allowed power laws of the coupling terms (exponent α in eq. (2)) as a function of the lattice dimension d . For the

d	$\text{Re}[A_d]$	$\text{Im}[A_d]$	b_d	c_d	$g_d(\cdot)$
1	≥ 0	$= 0$	$\frac{1}{2}$	1	$\cos(\cdot)$
2	≥ 0	$= 0$	$\frac{1}{\sqrt{\pi}}$	$\sqrt{2\pi}$	$\cos(\cdot)$
3	$= 0$	≤ 0	$\sqrt[3]{\frac{3}{4\pi}}$	$2\pi \cdot \sin^2 \vartheta$	$\sin(\cdot)$

Table 1. **Dimension-dependent quantities.** The table summarises the quantities appearing in eqs. (4), (13), (14), and (16)–(19) as function of the system dimension d for the three considered example cases. Here, $\vartheta = \arccos(\mathbf{k}\hat{\mathbf{e}}_{x_3}/k)$ denotes the angle between the eigenstate's wavevector \mathbf{k} and the x_3 axis.

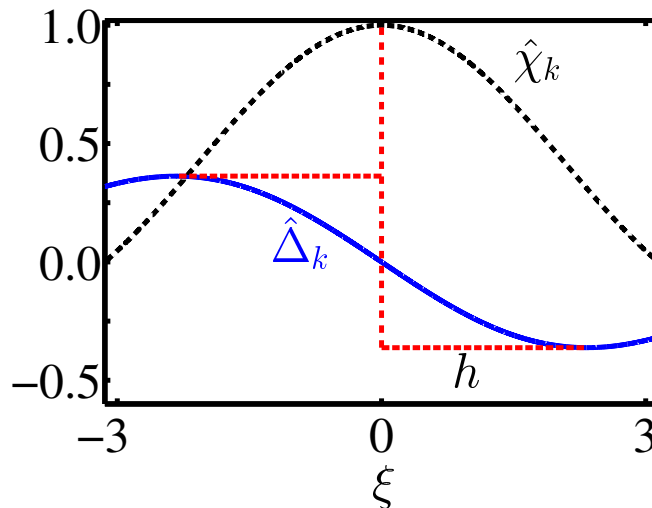


Figure 2. **Collective decay rates and frequency shifts.** Decay rates (black dashed curve) and frequency shifts (blue solid curve) as function of the wavenumber for $\alpha = (d-1)/2$. The figure is valid independent of dimensionality and coupling type, due to the scaling of decay rate $\hat{\chi}_k \equiv (\chi_k - 1)/(\chi_{\max} - 1)$, shift $\hat{\Delta}_k \equiv [(\Delta_k - \delta\omega_0)/\gamma_0]/[\epsilon(\chi_{\max} - 1)]$ and wavenumber $\xi \equiv (k - k_0)ab_d \sqrt[d]{N}$. Note the offset h between the extrema of the frequency shift and the decay rate maximum.

remainder, we assume that eq. (3) is satisfied. The enhancement factor χ_{\max} is (see table 1 for quantities b_d and c_d , and methods for the prefactor $L_d(\alpha)$)

$$\chi_{\max} \equiv \chi_{k=k_0} = 1 + \frac{|A_d| c_d (b_d)^{\frac{d+1}{2}-\alpha}}{\frac{d+1}{2}-\alpha} (k_0 a)^{\frac{1-d}{2}-\alpha} \sqrt[d]{N}^{\frac{d+1}{2}-\alpha} \quad (4)$$

$$= 1 + L_d(\alpha) \cdot \left(\frac{\lambda_0}{\sqrt[d]{\mathcal{V}}} \right)^{\frac{1}{2}(d-1)+\alpha} \cdot N. \quad (5)$$

In contrast to the maximum collective decay rate, we find that the collective frequency shift at $k = k_0$ is always zero independent of the actual physical realisation. We thus conclude that the case of maximum superradiance is unsuitable for a control of both collective decay rates and frequency shifts.

To circumvent this problem, we also consider states with wavenumbers around $k = k_0$. Indeed, for a large but finite system, also states with a wavenumber close to k_0 can exhibit an enhanced decay rate. We illustrate this for the most relevant case $\alpha = (d-1)/2$ (which includes the three common implementations mentioned below eq. (2)). For $|k - k_0|a \ll 1$, we find

$$\frac{\Gamma_k}{\gamma_0} = \chi_k \simeq 1 + (\chi_{\max} - 1) \cdot \text{sinc}(\xi), \quad (6)$$

$$\frac{\Delta_k - \delta\omega_0}{\gamma_0} \simeq \epsilon \cdot \frac{\chi_{\max} - 1}{2} \cdot \frac{\cos(\xi) - 1}{\xi}, \quad (7)$$

where $\xi \equiv (k - k_0)ab_d \sqrt[d]{N}$ and $\text{sinc}(\xi) \equiv \sin(\xi)/\xi$. Results are shown in fig. 2, scaled in such a way that they encompass different dimensions and coupling types. As mentioned before, those states which are maximally superradiant at $k = k_0$ do not exhibit a collective frequency shift. Rather, the frequency shift's first two extrema around k_0 occur at wavenumbers $k_{\pm} \equiv k_0 \pm h/(ab_d \sqrt[d]{N})$ (where $h \simeq 2.3311$). This finding represents a unique feature as it is independent of the actual realisation and provides a signature suitable for a direct experimental test.

Equations (6) and (7) also offer means to design an artificial optical transition with desired decay rate and frequency shift. In fact, the enhancement factor χ_{\max} represents a characteristic scale for both decay rates and frequency shifts. As expected, we find that the particle number N and/or the sample volume \mathcal{V} can be used to control χ_{\max} . But additionally, eqs. (4) and (5) explain how the dimensionality d , the type of the inter-atomic coupling as described by α , as well as the coupling strength to the environment can be used to manipulate the enhancement factor. This is of particular relevance, since these parameters could also be tuned *in situ* [10, 30]. However, as mentioned previously, these quantities are not sufficient to change the ratio between decay rate and frequency shift. This only becomes possible by also controlling the wave number k (see fig. 2). Experimentally, the wavenumber could be adjusted via the excitation angle of the probing light field.

From a broader perspective, our results also enable us to understand how superradiant states from different realisations can be compared and categorised. This is important, e. g., if superradiant ensembles realised using different individual constituents are to be combined to an effective artificial quantum system. To this end, suppose that we can control the atom number and the volume such that $N \rightarrow \tilde{N} \equiv f_N N$ and $\mathcal{V} \rightarrow \tilde{\mathcal{V}} \equiv f_V \mathcal{V}$, respectively, where f_N and f_V are arbitrary positive real numbers. Under this transformation, the enhancement factor changes as

$$\chi_{\max} \rightarrow \tilde{\chi}_{\max} = f_N \sqrt[d]{f_V}^{\frac{1}{2}(1-d-2\alpha)} \chi_{\max}. \quad (8)$$

This behaviour allows us to classify superradiant states from systems with different dimensionality and types of coupling. For instance, we may say that two extended samples characterised by (d, α) and (d', α') , respectively, are similar if they satisfy the same transformation rule (8) (leading to $(\alpha - 1/2)/d = (\alpha' - 1/2)/d'$). As an example, if a one-dimensional system ($d' = 1$) should “imitate” the superradiant state from three-dimensional free space ($d = 3, \alpha = 1$), the electromagnetic environment would have to be “engineered” [10] such that $\alpha' = 2/3$. Similarly, if an extended sample should realise small-volume superradiance, transformation (8) must reproduce the transformation of a Dicke system, which is simply $\chi_{\text{Dicke}} \rightarrow \tilde{\chi}_{\text{Dicke}}$ with $\chi_{\text{Dicke}} = N$ and $\tilde{\chi}_{\text{Dicke}} = \tilde{N} = f_N \chi_{\text{Dicke}}$. Hence, $\alpha = (1 - d)/2 \geq 0$, which reveals that only extended samples in one dimension ($d = 1$, otherwise we would have $\alpha < 0$) can behave “Dicke-like”.

In conclusion, we have studied single-photon superradiance in extended media, and showed how superradiance can be engineered in such a way that an artificial optical transition with tunable decay rate and level shift is realised. This result provides the basic building block for a systematic approach towards engineering advanced artificial quantum systems via superradiance by design. A promising avenue for future studies is the extension of our work to coupled sub ensembles with the goal to design artificial multi-level atoms [13].

METHODS

For an extended lattice, the plane wave ansatz $\varphi_{\mathbf{r}} = (1/\sqrt{N})e^{i\mathbf{k}\mathbf{r}}$ for eq. (1) yields the eigenstates’ decay rates $\Gamma_{\mathbf{k}} = -2\text{Im}(E_{\mathbf{k}})$ and frequency shifts $\Delta_{\mathbf{k}} = \text{Re}(E_{\mathbf{k}}) - \omega_0$ as

$$\Gamma_{\mathbf{k}} = \gamma_0 + \text{Re}[\mathcal{I}_d(\mathbf{k})], \quad (9)$$

$$\Delta_{\mathbf{k}} = \delta\omega_0 + \frac{1}{2}\text{Im}[\mathcal{I}_d(\mathbf{k})], \quad (10)$$

$$\mathcal{I}_d(\mathbf{k}) = \sum_{\mathbf{r}}' V_r e^{-i\mathbf{k}\mathbf{r}}. \quad (11)$$

Here, $\mathbf{r} = (x_1, \dots, x_d)^T$ denotes a d -dimensional lattice vector with components $x_i = an_i, i = 1, \dots, d, n_i = -\sqrt[d]{N}/2 + 1, \dots, \sqrt[d]{N}/2$, and $\sqrt[d]{N}$ is even. Likewise, $\mathbf{k} = (k_1, \dots, k_d)^T$ is the wavevector of the collective atomic excitation. The sum runs over all combinations of $\{n_i\}$ except $n_1 = \dots = n_d = 0$ and the couplings depend on the distance $r = |\mathbf{r}| = a\sqrt{n_1^2 + \dots + n_d^2}$ between atoms. We assume the atomic dipole moments to be uniformly aligned along the x_3 axis (e. g., by applying a weak magnetic field). Thus, for $d = 1, 2$ the distance vector \mathbf{r} (in the x_1 - x_2 plane) is perpendicular to the dipole moments, and for $d = 3$ we have to take into account the polar angle $\theta = \arccos(x_3/r)$. Furthermore, we make use of the assumptions $N \gg 1$ (many atoms) and $k_0 a > 1$ (extended sample). The decay rate eq. (9) can also be rewritten in terms of the enhancement factor

$$\chi_{\mathbf{k}} \equiv \frac{\Gamma_{\mathbf{k}}}{\gamma_0} = 1 + \frac{\text{Re}[\mathcal{I}_d(\mathbf{k})]}{\gamma_0}. \quad (12)$$

To arrive at the final expressions eqs. (4)-(7), we further manipulate eqs. (9)-(12) as follows. In this paper, we focus on the system’s eigenstates and—to keep the analysis general—do not consider geometric details or questions of how to excite and probe the system since such details vary from experiment to experiment. Around $k \equiv |\mathbf{k}| = k_0$, we can utilise a continuum formulation, rewrite the lattice sums in eq. (11) into an integral, and perform the angular integration for couplings of type (2) (see supplementary information for further technical details of the calculation),

leading to

$$\frac{\mathcal{I}_d}{\gamma_0} = \frac{2c_d}{(k_0 a)^d} \cdot \left(\frac{k_0}{k}\right)^{\frac{1}{2}(d-1)} \cdot A_d \cdot \mathcal{J}_d(k), \quad (13)$$

$$\mathcal{J}_d(k) = \int_{k_0 a}^{k_0 a b_d \sqrt[d]{N}} d\eta e^{i\eta} g_d(k k_0^{-1} \eta) \eta^\beta, \quad (14)$$

$$\beta \equiv \frac{d-1}{2} - \alpha. \quad (15)$$

The dimension-dependent quantities A_d , b_d , c_d , and g_d are listed in table 1 (for instance, A_d is real for $d = 1, 2$ and purely imaginary for $d = 3$). Note that the factor $\exp(\pm i k_0 r)$ from eq. (2) in the eigenproblem (1) can be understood as a radial translation in wavenumber space. In the shifted frame, a long-wavelength limit of the collective atomic excitation (which can be accounted for by a continuum description) corresponds to $k \rightarrow k_0$. This continuum formulation is applicable in the range $|k - k_0| \lesssim \pi / a b_d \sqrt[d]{N}$. Further, in eq. (2), we have not included exponential damping of the form $\exp(-k_0 r / \ell)$, where ℓ denotes a dimensionless absorption length that, for instance, empirically accounts for material imperfections. Such a damping factor in the integral in eq. (14) would lead to a broadening and modification of the $k = k_0$ -criterion for maximal superradiance, going beyond the scope of this paper. Details on the calculation of the integrals in eq. (14) can be found in the supplementary material.

The maximum enhancement factor (4) can be cast into the equivalent forms ($\mathcal{V} = N a^d$ denotes the sample volume, $\rho = N / \mathcal{V}$ is the number density, and $\chi_{\max} - 1 \simeq \chi_{\max}$ since $N \gg 1$)

$$\frac{\chi_{\max}}{L_d(\alpha)} = \left(\frac{\lambda_0}{\sqrt[d]{\mathcal{V}}}\right)^{\frac{1}{2}(d-1)+\alpha} \cdot N \quad (N, \mathcal{V}) \quad (16)$$

$$= \left(\frac{\lambda_0}{\sqrt[d]{\mathcal{V}}}\right)^{\frac{1}{2}(d-1)+\alpha} \cdot \mathcal{V} \cdot \rho \quad (\mathcal{V}, \rho) \quad (17)$$

$$= (\lambda_0 \sqrt[d]{\rho})^{\frac{1}{2}(d-1)+\alpha} \cdot \sqrt[d]{N}^{\frac{1}{2}(d+1)-\alpha} \quad (N, \rho), \quad (18)$$

$$L_d(\alpha) \equiv \frac{2(b_d)^{\frac{1}{2}(d+1)-\alpha} c_d}{d+1-2\alpha} \cdot \frac{|A_d|}{(2\pi)^{\frac{1}{2}(d-1)+\alpha}}. \quad (19)$$

Which formulation to choose from eqs. (16)-(18) depends on which quantities can be controlled in an experiment.

If for small volumes the length scale set by the inter-atomic distance a is effectively eliminated from the single-excitation eigenproblem (1) (possibly neglecting divergent contributions to the inter-atomic coupling [2, 31]), all atoms couple to each other with equal strength V_0 . The resulting equation $E - \omega_0 = -(i/2)V_0 \sum_{j=1}^N \varphi_{\mathbf{r}_j} / \varphi_{\mathbf{r}_i}$ (which must hold for all \mathbf{r}_i) yields a maximal decay rate for a spatially constant wavefunction with equal relative phase between all atom pairs, representing the maximally symmetric Dicke state. For this state, $\Gamma = -2\text{Im}(E) = N\gamma_0$ and $\Delta = \text{Re}(E) - \omega_0 = N\delta\omega_0$.

- [1] Dicke, R. H. Coherence in spontaneous radiation processes. *Phys. Rev.* **93**, 99-110 (1954).
- [2] Gross, M. & Haroche, S. Superradiance: An essay on the theory of collective spontaneous emission. *Phys. Rep.* **93**, 301-396 (1982).
- [3] Friedberg, R., Hartmann, S. R. & Manassah, J. T. Frequency shifts in emission and absorption by resonant systems of two-level atoms. *Phys. Rep.* **7**, 101-179 (1973).
- [4] Friedberg, R. & Manassah, J. T. The dynamical cooperative Lamb shift in a system of two-level atoms in a slab-geometry. *Phys. Lett. A* **373**, 3423-3429 (2009).
- [5] Scully, M. O. & Svidzinsky, A. A. The super of superradiance. *Science* **325**, 1510-1511 (2009).
- [6] Kien, F. L., Gupta, S. D., Nayak, K. P., & Hakuta, K. Nanofiber-mediated radiative transfer between two distant atoms. *Phys. Rev. A* **72**, 063815; DOI:10.1103/PhysRevA.72.063815 (2005).
- [7] Keaveney, J. et al. Cooperative Lamb shift in an atomic vapor layer of nanometer thickness. *Phys. Rev. Lett.* **108**, 173601; DOI:10.1103/PhysRevLett.108.173601 (2012).

- [8] Pellegrino, J. et al. Observation of suppression of light scattering induced by dipole-dipole interactions in a cold atomic ensemble. *Phys. Rev. Lett.* **113**, 133602; DOI:10.1103/PhysRevLett.113.133602 (2014).
- [9] Meir, Z., Schwartz, O., Shahmoon, E., Oron, D., & Ozeri, R. Cooperative Lamb shift in a mesoscopic atomic array. *Phys. Rev. Lett.* **113**, 193002; DOI:10.1103/PhysRevLett.113.193002 (2014).
- [10] Douglas, J. S. et al. Quantum many-body models with cold atoms coupled to photonic crystals. *Nat. Photonics* **9**, 326-331 (2015).
- [11] Akkermans, E., Gero, A. & Kaiser, R. Photon localization and Dicke superradiance in atomic gases. *Phys. Rev. Lett.* **101**, 103602; DOI:10.1103/PhysRevLett.101.103602 (2008).
- [12] Javanainen, J., Ruostekoski, J., Li, Y. & Yoo, S.-M. Shifts of a resonance line in a dense atomic sample. *Phys. Rev. Lett.* **112**, 113603; DOI:10.1103/PhysRevLett.112.113603 (2014).
- [13] Röhlberger, R., Wille, H.-C., Schlage, K. & Sahoo, B. Electromagnetically induced transparency with resonant nuclei in a cavity. *Nature* **482**, 199-203 (2012).
- [14] Heeg, K. P. et al. Vacuum-assisted generation and control of atomic coherences at x-ray energies. *Phys. Rev. Lett.* **111**, 073601; DOI:10.1103/PhysRevLett.111.073601 (2013).
- [15] Heeg, K. P. et al. Tunable subluminal propagation of narrow-band x-ray pulses. *Phys. Rev. Lett.* **114**, 203601; DOI:10.1103/PhysRevLett.114.203601 (2015).
- [16] Röhlberger, R., Schlage, K., Sahoo, B., Couet, D. & Ruffer, R. Collective Lamb shift in single-photon superradiance. *Science* **328**, 1248-1251 (2010).
- [17] Heeg, K. P. et al. Interferometric phase detection at x-ray energies via Fano resonance control. *Phys. Rev. Lett.* **114**, 207401; DOI:10.1103/PhysRevLett.114.207401 (2015).
- [18] Heeg, K. P. & Evers, J. X-ray quantum optics with Mössbauer nuclei embedded in thin-film cavities. *Phys. Rev. A* **88**, 043828; DOI:10.1103/PhysRevA.88.043828 (2013).
- [19] Vagizov, F., Antonov, V., Radeonychev, Y. V., Shakhmuratov, R. N. & Kocharovskaya, O. Coherent control of the waveforms of recoilless γ -ray photons. *Nature* **508**, 80-83 (2014).
- [20] Adams, B. W. et al. X-ray quantum optics. *J. Mod. Opt.* **60**, 2-21 (2013).
- [21] Ficek, Z. & Swain, S. *Quantum interference and coherence* (Springer, New York, 2005).
- [22] Li, Y., Evers, J., Zheng, H. & Zhu, S.-Y. Collective spontaneous emission beyond the rotating-wave approximation. *Phys. Rev. A* **85**, 053830; DOI:10.1103/PhysRevA.85.053830 (2012).
- [23] Longo, P. & Evers, J. Far-field signatures of a two-body bound state in collective emission from interacting two-level atoms on a lattice. *Phys. Rev. Lett.* **112**, 193601; DOI:10.1103/PhysRevLett.112.193601 (2014).
- [24] Longo, P. & Evers, J. Probing few-excitation eigenstates of interacting atoms on a lattice by observing their collective light emission in the far field. *Phys. Rev. A* **90**, 063834; DOI:10.1103/PhysRevA.90.063834 (2014).
- [25] Agarwal, G. S. *Quantum statistical theories of spontaneous emission and their relation to other approaches* (Springer, Berlin, 1974).
- [26] Jaksch, D. & Zoller, P. The cold atom Hubbard toolbox. *Ann. Phys.* **315**, 52-79 (2005).
- [27] Kay, A. & Angelakis, D.G. Reproducing spin lattice models in strongly coupled atom-cavity systems. *Europhys. Lett.* **84**, 20001; DOI:10.1209/0295-5075/84/20001 (2008).
- [28] Couto, R. T. Green's functions for the wave, Helmholtz and Poisson equations in a two-dimensional boundless domain. *Rev. Bras. Ensino Fis.* **35**, 1304; DOI:10.1590/S1806-11172013000100004 (2013).
- [29] Gonzalez-Tudela, A. et al. Entanglement of two qubits mediated by one-dimensional plasmonic waveguides. *Phys. Rev. Lett.* **106**, 020501; DOI:10.1103/PhysRevLett.106.020501 (2011).
- [30] Goban, A. et al. Atom-light interactions in photonic crystals. *Nat. Commun.* **5**, 3808; DOI:10.1038/ncomms4808 (2014).
- [31] Garraway, B. M. The Dicke model in quantum optics: Dicke model revisited. *Philos. Trans. R. Soc., A* **369**, 1137-1155 (2011).

AUTHOR CONTRIBUTIONS

P.L. initiated the project, performed the calculations, and, together with J.E., interpreted the results. P.L. and J.E. wrote the manuscript. All authors contributed to the development of ideas, critical discussions, and the preparation of the manuscript. C.K. and J.E. guided the project.

COMPETING FINANCIAL INTERESTS

The authors declare no competing financial interests.

SUPPLEMENTARY INFORMATION

In this supplementary information, we provide technical details on how to rewrite the lattice sums into an integral and on how to ultimately perform the integration.

I. $\mathcal{I}_d(\mathbf{k})$

The quantity

$$\mathcal{I}_d(\mathbf{k}) = \sum'_{n_1} \cdots \sum'_{n_d} V_{a\sqrt{n_1^2 + \cdots + n_d^2}} e^{-ik_1 a n_1} \cdots e^{-ik_d a n_d}, \quad (20)$$

where the sums run over all combinations of $\{n_i\}$ except $n_1 = \cdots = n_d = 0$, can be rewritten into an integral

$$\mathcal{I}_d(\mathbf{k}) \rightarrow \int \frac{d^d x}{a^d} V(r, \theta) \prod_{j=1}^d e^{-k_j x_j}. \quad (21)$$

For $d = 1, 2$, $V(r, \theta) = f_r$, whereas for $d = 3$, $V(r, \theta) = \sin^2 \theta f_r$ ($f_r \equiv A_d \exp(ik_0 r)/(k_0 r)^\alpha$). Here, $d^d x$ signifies the d dimensional infinitesimal volume element and the integration is over all space except for a region with radius a around the origin ($d^1 x = dx$, $d^2 x = r dr d\varphi$, $d^3 x = r^2 \sin \theta dr d\varphi d\theta$).

Explicitly, for $d = 1$,

$$\begin{aligned} \mathcal{I}_1 &= \int_{-\frac{Na}{2}}^{\frac{Na}{2}} \frac{dx}{a} \Theta(|x| - a) f_{|x|} e^{-ikx} \\ &= \int_a^{\frac{Na}{2}} \frac{dx}{a} f_{|x|} 2 \cos(kx) \\ &= 2 \int_a^{\frac{Na}{2}} \frac{dr}{a} f_r \cos(kr), \end{aligned} \quad (22)$$

where $k = |\mathbf{k}|$ and $\Theta(\cdot)$ signifies the Heaviside step function. For $d = 2$,

$$\begin{aligned} \mathcal{I}_2 &= \int_a^{N'_2 a} \int_0^{2\pi} \frac{r dr d\varphi}{a^2} f_r e^{-ik_1 r \cos \varphi} e^{-ik_2 r \sin \varphi} \\ &= \frac{2\pi}{a^2} \int_a^{N'_2 a} dr r f_r J_0(kr), \end{aligned} \quad (23)$$

where N'_2 is chosen such that the integration area covers N atoms, i. e., $\pi(N'_2)^2 = N$. For $d = 3$,

$$\begin{aligned} \mathcal{I}_3 &= \int_a^{N'_3 a} \frac{r^2 dr}{a^3} \int_0^\pi d\theta \sin \theta \int_0^{2\pi} d\varphi \underbrace{V(r, \theta)}_{=\sin^2 \theta f_r} \\ &\quad \times e^{-ik_1 r \sin \theta \cos \varphi} e^{-ik_2 r \sin \theta \sin \varphi} e^{-ik_3 r \cos \theta} \\ &= 2\pi \int_a^{N'_3 a} \frac{r^2 dr}{a^3} f_r \int_0^\pi d\theta \sin^3 \theta e^{-ik_3 r \cos \theta} \\ &\quad \times J_0 \left(\sin \theta \sqrt{k_1^2 + k_2^2} r \right), \end{aligned} \quad (24)$$

where $(4\pi/3)(N'_3)^3 = N$, $J_0(\cdot)$ signifies the zeroth-order Bessel function of first kind, and $\text{sinc}(x) = \sin(x)/x$. The integration over θ can be done as follows. Upon defining $I_m \equiv \int_0^\pi d\theta \sin^m \theta \exp(-ik_\perp r \cos \theta) J_0(k_\parallel r \sin \theta)$, $k_\perp \equiv k_3$, and $k_\parallel \equiv \sqrt{k_1^2 + k_2^2}$, we have the relation

$$\begin{aligned} I_3 &= I_1 - \int_0^\pi d\theta \cos^2 \theta \sin \theta e^{-ik_\perp r \cos \theta} J_0(k_\parallel r \sin \theta) \\ &= \left(1 + \frac{1}{r^2} \frac{\partial^2}{\partial k_\perp^2} \right) I_1. \end{aligned} \quad (25)$$

To simplify the integration needed for I_1 , we can choose a coordinate system in which either $k_{\perp} = 0$ or $k_{\parallel} = 0$ (it can be shown that I_1 does not depend on the orientation of \mathbf{k}), yielding

$$I_1 = 2 \operatorname{sinc} \left(\sqrt{k_{\perp}^2 + k_{\parallel}^2} r \right). \quad (26)$$

Finally, $I_3 = \sin^2 \vartheta \cdot 2\operatorname{sinc}(kr) + \mathcal{O}[(kr)^{-2}]$ and therefore

$$\mathcal{I}_3 = \frac{4\pi}{a^3} \sin^2 \vartheta \int_a^{N'_3 a} dr r^2 f_r \operatorname{sinc}(kr), \quad (27)$$

where ϑ denotes the angle between the eigenstate's wavevector \mathbf{k} and the z axis. Here, we have only taken into account the asymptotic leading order term (with respect to kr). Other terms can be accounted for by means of different coefficients α (see main text). Introducing the abbreviations used in the paper and performing a variable substitution, we finally arrive at the integrals $\mathcal{J}_d(k)$ (Eq. (14) in the main text).

II. $\mathcal{J}_d(k)$

We now proceed with the radial integration

$$\mathcal{J}_d(k) = \int_{k_0 a}^{k_0 a b_d \sqrt[d]{N}} d\eta e^{\pm i\eta} g_d(k k_0^{-1} \eta) \eta^{\beta}. \quad (28)$$

Note that for $d = 2$ the integration kernel is actually given by $J_0(k k_0^{-1} \eta)$. However, already at the lower integration limit, we can use the asymptotic form $J_0(ka) \approx \sqrt{2/\pi} \cos(ka - \pi/4)/\sqrt{ka}$ since in an extended sample $k_0 a > 1$ and only the wavenumbers k around k_0 are relevant. Furthermore, by an additional substitution of the integration variable, we shift the $\pi/4$ shift to the argument to the exponential (which we can account for by means of appropriate prefactors), $\eta + \pi/4 \approx \eta$, and the integration limits can also approximately remain unchanged.

The possible combinations in the integrand we need to consider are

$$J_{cc} \equiv \int_{k_0 a}^{k_0 a b_d \sqrt[d]{N}} d\eta \cos(\eta) \cos(k k_0^{-1} \eta) \eta^{\beta}, \quad (29)$$

$$J_{sc} \equiv \int_{k_0 a}^{k_0 a b_d \sqrt[d]{N}} d\eta \sin(\eta) \cos(k k_0^{-1} \eta) \eta^{\beta}, \quad (30)$$

$$J_{cs} \equiv \int_{k_0 a}^{k_0 a b_d \sqrt[d]{N}} d\eta \cos(\eta) \sin(k k_0^{-1} \eta) \eta^{\beta}, \quad (31)$$

$$J_{ss} \equiv \int_{k_0 a}^{k_0 a b_d \sqrt[d]{N}} d\eta \sin(\eta) \sin(k k_0^{-1} \eta) \eta^{\beta}. \quad (32)$$

A. J_{cc}

Utilizing a computer algebra system, we find that

$$J_{cc} = \frac{i^{\beta+1}}{4} \cdot \left[\left(\frac{r_-}{k_0} \right)^{-1-\beta} (\operatorname{sgn}(r_-))^{-2\beta} \right. \\ \left. \times \left(\Gamma(1 + \beta, -ir_- a) \right. \right. \\ \left. \left. - \Gamma(1 + \beta, -ir_- a N'_d) \right) \right] \quad (33)$$

$$\begin{aligned}
& - (-1)^\beta \Gamma(1 + \beta, ir_- a) \\
& + (-1)^\beta \Gamma(1 + \beta, ir_- a N'_d) \\
& + \left(\frac{r_+}{k_0} \right)^{-1-\beta} \\
& \times \left(\Gamma(1 + \beta, -ir_+ a) \right. \\
& \quad - \Gamma(1 + \beta, -ir_+ a N'_d) \\
& \quad - (-1)^\beta \Gamma(1 + \beta, ir_+ a) \\
& \quad \left. + (-1)^\beta \Gamma(1 + \beta, ir_+ a N'_d) \right),
\end{aligned}$$

where $r_\pm \equiv k \pm k_0$ and $\Gamma(a, z) \equiv \int_z^\infty dt t^{a-1} e^{-t}$ signifies the incomplete Gamma function. The asymptotic form for $N'_d \gg 1$ and $r_- \neq 0$ reads

$$\begin{aligned}
J_{cc}(k \neq k_0) & \simeq \frac{i^{\beta+1}}{4} \cdot \left[\left(\frac{r_-}{k_0} \right)^{-1-\beta} (\text{sgn}(r_-))^{-2\beta} \right. \\
& \quad \times \left(\Gamma(1 + \beta, -ir_- a) \right. \\
& \quad \quad - (-1)^\beta \Gamma(1 + \beta, ir_- a) \\
& \quad \quad \left. - 2i(-1)^\beta (ir_- a N'_d)^\beta \sin(ir_- a N'_d) \right) \\
& + \left(\frac{r_+}{k_0} \right)^{-1-\beta} \\
& \quad \times \left(\Gamma(1 + \beta, -ir_+ a) \right. \\
& \quad \quad - (-1)^\beta \Gamma(1 + \beta, ir_+ a) \\
& \quad \quad \left. - 2i(-1)^\beta (ir_+ a N'_d)^\beta \sin(ir_+ a N'_d) \right).
\end{aligned} \tag{34}$$

The dominant terms for $N'_d \gg 1$ in this expression are $\propto (N'_d)^\beta$ if $\beta > 0$.

For $k \rightarrow k_0$ ($N'_d = b_d \sqrt[4]{N} \gg 1$), we arrive at

$$J_{cc}(k \rightarrow k_0) \simeq \frac{1}{2(1+\beta)} (k_0 a)^{\beta+1} (N'_d)^{\beta+1} \tag{35}$$

$$= \frac{(b_d)^{\beta+1}}{2(1+\beta)} (k_0 a)^{\beta+1} N^{\frac{\beta+1}{4}}. \tag{36}$$

Here, the dominant terms for $N'_d \gg 1$ are $\propto (N'_d)^{\beta+1}$ if $\beta > -1$.

For the case $\beta = 0$, the explicit expression for the integral reads

$$\begin{aligned}
J_{cc} & \stackrel{\beta=0}{=} \frac{k_0 a}{2} \left[N'_d (\text{sinc}(r_- a N'_d) + \text{sinc}(r_+ a N'_d)) \right. \\
& \quad \left. - \text{sinc}(r_+ a) - \text{sinc}(r_- a) \right] \\
& \stackrel{|r_-| a \ll 1, N'_d \gg 1}{\simeq} \frac{k_0 a}{2} N'_d \text{sinc}(r_- a N'_d) \\
& \stackrel{k \rightarrow k_0}{\rightarrow} \frac{k_0 a}{2} N'_d = \frac{k_0 a}{2} b_d N^{\frac{1}{4}}.
\end{aligned} \tag{37}$$

In the second step, we focus on wavenumbers k around k_0 (i. e., small $|r_-| a$, for which the terms with r_+ are negligible).

B. J_{sc}

Similarly,

$$\begin{aligned}
J_{sc} = \frac{i^{\beta+2}}{4} \cdot & \left[\left(\frac{r_-}{k_0} \right)^{-1-\beta} (\text{sgn}(r_-))^{-2\beta} \right. \\
& \times \left(-\Gamma(1+\beta, -ir_-a) \right. \\
& \quad + \Gamma(1+\beta, -ir_-aN'_d) \\
& \quad - (-1)^\beta \Gamma(1+\beta, ir_-a) \\
& \quad \left. + (-1)^\beta \Gamma(1+\beta, ir_-aN'_d) \right) \\
& + \left(\frac{r_+}{k_0} \right)^{-1-\beta} \left(\Gamma(1+\beta, -ir_+a) \right. \\
& \quad - \Gamma(1+\beta, -ir_+aN'_d) \\
& \quad + (-1)^\beta \Gamma(1+\beta, ir_+a) \\
& \quad \left. - (-1)^\beta \Gamma(1+\beta, ir_+aN'_d) \right) \left. \right]. \tag{38}
\end{aligned}$$

The asymptotic form for $N'_d \gg 1$ but $r_- \neq 0$ reads

$$\begin{aligned}
J_{sc}(k \neq k_0) \simeq \frac{i^{\beta+2}}{4} \cdot & \left[\left(\frac{r_-}{k_0} \right)^{-1-\beta} (\text{sgn}(r_-))^{-2\beta} \right. \\
& \times \left(-\Gamma(1+\beta, -ir_-a) \right. \\
& \quad - (-1)^\beta \Gamma(1+\beta, ir_-a) \\
& \quad + 2(-1)^\beta (ir_-aN'_d)^\beta \cos(r_-aN'_d) \Big) \\
& + \left(\frac{r_+}{k_0} \right)^{-1-\beta} \left(\Gamma(1+\beta, -ir_+a) \right. \\
& \quad - (-1)^\beta \Gamma(1+\beta, ir_+a) \\
& \quad \left. - 2(-1)^\beta (ir_+aN'_d)^\beta \cos(r_+aN'_d) \right) \left. \right]. \tag{39}
\end{aligned}$$

In contrast to the integral J_{cc} , the limit $k \rightarrow k_0$ does not yield a scaling $\propto (N'_d)^{\beta+1}$. The case $\beta = 0$ reads

$$\begin{aligned}
J_{sc} \stackrel{\beta=0}{=} & \frac{k_0 a}{2} \left[\frac{\cos(r_-aN'_d)}{r_-a} - \frac{\cos(r_+aN'_d)}{r_+a} \right. \\
& \quad \left. - \frac{\cos(r_-a)}{r_-a} + \frac{\cos(r_+a)}{r_+a} \right] \\
\stackrel{|r_-|a \ll 1}{\simeq} & \frac{k_0 a}{2} \cdot \frac{\cos(r_-aN'_d) - 1}{r_-a}. \tag{40}
\end{aligned}$$

C. J_{cs}

We can rewrite

$$\begin{aligned}
J_{cs} &= \int_{k_0 a}^{k_0 a b_d \sqrt[4]{N}} d\eta \cos(\eta) \sin(k k_0^{-1} \eta) \eta^\beta \\
&= \left(\frac{k_0}{k} \right)^{\beta+1} \int_{ka}^{kab_d \sqrt[4]{N}} d\eta \sin(\eta) \cos(k_0 k^{-1} \eta) \eta^\beta. \tag{41}
\end{aligned}$$

This is in essence just the integral J_{sc} with k and k_0 interchanged. In particular, for $\beta = 0$, $J_{cs} = -J_{sc}$.

D. J_{ss}

For $k \rightarrow k_0$, we can write

$$\begin{aligned}
 J_{ss}(k \rightarrow k_0) &= \int_{k_0 a}^{k_0 a b_d \sqrt[4]{N}} d\eta (1 - \cos^2 \eta) \eta^{\beta+1} \\
 &= \underbrace{(k_0 a b_d \sqrt[4]{N})^{\beta+1} - (k_0 a)^{\beta+1}}_{2J_{cc}(k \rightarrow k_0)} - J_{cc}(k \rightarrow k_0) \\
 &\stackrel{N \gg 1}{\simeq} J_{cc}(k \rightarrow k_0).
 \end{aligned} \tag{42}$$

For $\beta = 0$, the explicit expression reads

$$\begin{aligned}
 J_{ss} &\stackrel{\beta=0}{=} \frac{k_0 a}{2} \left[N'_d (\text{sinc}(r_- a N'_d) - \text{sinc}(r_+ a N'_d)) \right. \\
 &\quad \left. + \text{sinc}(r_+ a) - \text{sinc}(r_- a) \right] \\
 &\stackrel{|r_-| a \ll 1, N'_d \gg 1}{\simeq} \frac{k_0 a}{2} N'_d \text{sinc}(r_- a N'_d).
 \end{aligned} \tag{43}$$